

Technical Notes

TECHNICAL NOTES are short manuscripts describing new developments or important results of a preliminary nature. These Notes cannot exceed 6 manuscript pages and 3 figures; a page of text may be substituted for a figure and vice versa. After informal review by the editors, they may be published within a few months of the date of receipt. Style requirements are the same as for regular contributions (see inside back cover).

Distortion of a Turbulent Scalar Upstream of Axisymmetric Objects

Hamid R. Rahai*

California State University, Long Beach,
Long Beach, California 90840

and

John C. LaRue†

University of California, Irvine,
Irvine, California 92717

Nomenclature

- D = diameter of the axisymmetric objects, cm
 d = distorted (i.e., denotes quantities measured when objects are present)
 L_0 = integral length scale, cm
 $\overline{u_1^2}^{1/2}$ = streamwise root mean square turbulent velocity, m/s
 $\overline{u_1 \theta}$ = axial heat flux, m°C/s
 $\overline{\theta_1^2}^{1/2}$ = root mean square temperature, °C
 x_1 = streamwise distance measured upstream from the objects with origin at the stagnation point, cm
 y = transverse direction with origin at the stagnation point, cm

Introduction

THE distortion of a turbulent flow as it approaches an axisymmetric object is of both fundamental and practical interest. The latter is due to the fact that many probe supports are axisymmetric and many probe platforms such as aircraft or submarines are approximately so. Thus, an assessment of the effects of these objects on the measured turbulent quantities of interest is of importance.

Previous studies of the effect of the flow distortion caused by two-dimensional objects (Hunt,¹ Bearman,² Britter, et al.,³ and Rahai and LaRue⁴) have shown significantly different effects depending on whether the ratio of L_0 to D is very large or very small. When L_0/D is large, along the mean stagnation streamline, the root mean square (rms) velocity decreases in a manner similar to the mean velocity as the object is approached. However, when L_0/D is small, starting at about one diameter upstream of the object, the rms velocity initially increases due to the vortex stretching. Closer to the object (starting about one integral scale upstream of the object) the rms velocity begins to decrease. This decrease in the rms velocity is due to the blockage effect.

In contrast to the results for the velocity field, the rms temperature and temperature spectra for all L_0/D do not show any change outside the region where the blockage effect is important (cf. Rahai and LaRue⁴).

Wyngaard et al.⁵ study the effects of mean flow distortion caused by an axisymmetric object on the turbulence statistics when $L_0/D \gg 1$. In their study, a Taylor's series expansion and a flow distortion matrix which relates the velocity field near the object to the freestream velocity are used as a means of determining the effect of distortion on the turbulence statistics. Their results show that distortion can induce significant variation in the velocity covariances measured ahead of axisymmetric objects. The errors depend on the flow distortion matrix as well as on the freestream turbulence properties and, weakly, on the angle of attack. There appears to be no corresponding experimental studies for the axisymmetric case. In addition, for this case there appears to be neither analytical nor experimental studies of the effect of distortion on the turbulent passive scalar field. This provides the motivation for the study discussed herein.

Experimental Procedure and Techniques

The heated turbulent flow is produced in a wind tunnel by means of two biplane grids. The first consists of 0.254-mm-diam chromel- p wires which are electrically heated and has a solidity of 0.04. The temperature rise across the grid is 0.5°C. The heater grid is placed 99-cm downstream of the second biplane grid of polished aluminum rods which is placed 60-cm downstream of the exit of the contraction. Two biplane grids of polished aluminum rods are used in the study. One has a rod diameter of 0.476 cm with a mesh spacing 2.54 cm, while the second has a rod diameter of 0.95 cm with a mesh spacing of 5.08 cm. The solidity for both is 0.34.

All measurements are carried out in the UC Irvine closed circuit wind tunnel with a working area which has a cross-sectional width of 60 cm, a height of 90 cm, and a length of 6.7 m. The background intensity is 0.06%. The mean velocity is 5.6 m/s which corresponds to grid Reynolds numbers of 9300 and 18,600. The corresponding integral scales, 30.45-cm downstream of the heated grid, are 1.2 and 2.3 cm, respectively.

Two axisymmetric bodies are used in the study. Both are composed of tubes with diameters of 3.81 and 0.635 cm which are 40 cm in length with their axes aligned with the flow. Hemispherical noses are attached to the upstream end of the tubes which are mounted on a slender stand and placed inside the tunnel. The stagnation point on the hemisphere is 30 cm ahead of the stand.

Simultaneous time resolved measurement of the longitudinal velocity and temperature are obtained using a specially designed probe which consists of a TSI T1.5 hot wire and a cold wire which are mounted 1-mm apart. The tips of the probe support are constructed so that near the sensor the probe supports are parallel to the flow for a distance of 5 mm. The hot wire is operated in the constant temperature mode using a TSI Model 1050 anemometer at an overheat of 1.7. The cold wire is platinum, 0.625 μ m in diameter with a length of 0.75 mm and is operated at a rms current of 180 μ A using an ac Wheatstone bridge. The current supplied to the cold wire is low enough so that its sensitivity to velocity is insignificant (cf. LaRue et al.⁶). The probe is directly calibrated

Presented as Paper 90-1591 at the AIAA 21st Fluid Dynamics, Plasma Dynamics, and Lasers Conference, Seattle, WA, June 18–20, 1990; received Nov. 4, 1991; revision received May 7, 1992; accepted for publication May 27, 1992. Copyright © 1991 by the American Institute of Aeronautics and Astronautics, Inc. All rights reserved.

*Assistant Professor, Mechanical Engineering Department, 1250 Bellflower Blvd.

†Associate Professor, Mechanical and Aerospace Engineering Department. Member AIAA.

for velocity and temperature over the range of 3–9 m/s and 17–23°C. The frequency response of the hot wire, determined using the square wave technique, is 16 kHz and that of the cold wire is estimated to be about 4 kHz (cf. LaRue et al.⁶).

For measurements near the stagnation point, a similar probe with a vertical sensor support (normal to the flow) is used.

Experiments are carried out along $y = 0$ (the stagnation streamline) and $y = D/2$ (along a line parallel to the edge of the object). More details of the experimental arrangements and data reduction techniques are given by Rahai and LaRue.⁷

Results and Discussions

Figures 1a–c show the variation of the normalized rms velocity, rms temperature, and axial heat flux for different L_0/D ratios. When $L_0/D = 3.5$, starting at $x_1/D = 0.16$, the blockage effect causes the normalized rms velocity to decrease in a manner similar to the mean velocity. The value is reduced to 72% of the undistorted value at $x_1/D = 0.16$. When $L_0/D = 0.32$, vortex stretching effects cause the normalized rms velocity to increase starting at $x_1/D = 0.8$. The distorted value becomes 1.2 times the undistorted value at $x_1/D = 0.25$. Comparison between the results with the corresponding results from the two-dimensional objects (cf. Rahai and LaRue⁵)

shows that the distortion effect is less pronounced for axisymmetric objects. For example, in the two-dimensional case, when $L_0/D = 0.470$ and $x_1/D = 0.5$, the increase in the rms velocity is 10%. Contrast this with the increase of only 4% for the flow upstream of the axisymmetric object at $x_1/D = 0.5$ and $L_0/D = 0.32$.

When $L_0/D = 0.32$, the rms temperature does not change for $x_1/D \geq 0.25$. This is in contrast to the rms velocity which increases by 20% compared to the undistorted value at the same location.

The blockage effect becomes important at a distance from the surface which is approximately equal to the integral length scale or the body dimension, whichever is smaller. However, the blockage effect occurs closer to the stagnation point of the axisymmetric objects than for two-dimensional objects, and thus, its effect is observed relatively closer to the stagnation point than it is for the two-dimensional objects.

For $L_0/D = 3.5$, the normalized rms temperature does not change for $x_1/D \geq 0.5$. However, for $x_1/D < 0.5$, the normalized rms temperature decreases and becomes 98% of the undistorted value at $x_1/D = 0.16$.

It should be noted that although the strain due to the presence of the axisymmetric objects differ from the strain due to the presence of the two-dimensional objects, their effects

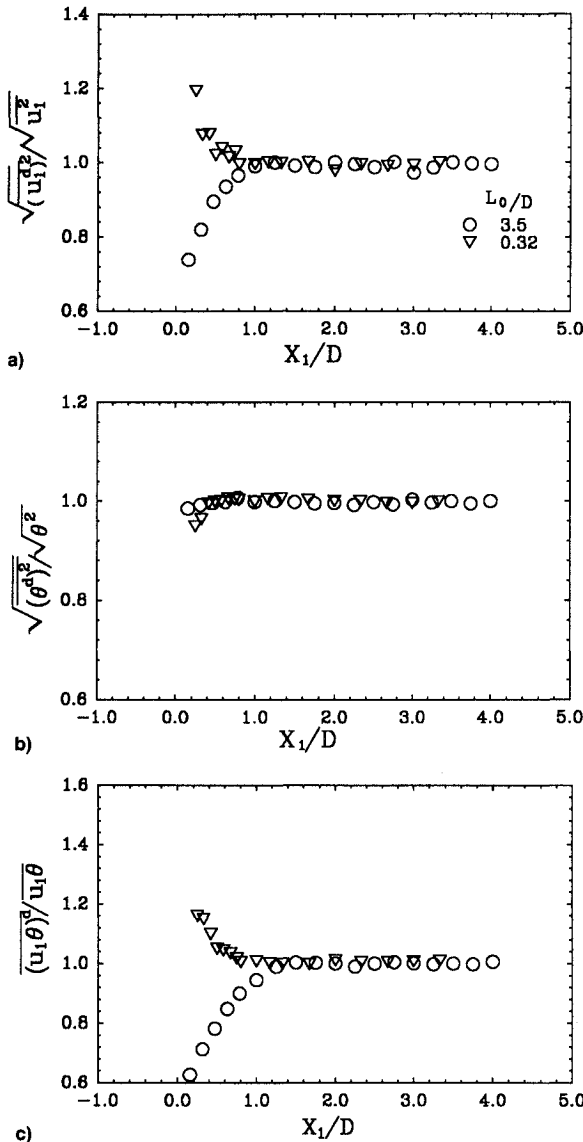


Fig. 1 Variation of the normalized a) rms velocity, b) rms temperature, and c) axial heat flux for flow along $y = 0$ (uncertainty in the normalized rms velocity is ± 0.02 , in the normalized rms temperature it is ± 0.03 , and in the x_1/D it is ± 0.05 at 20:1 odds).

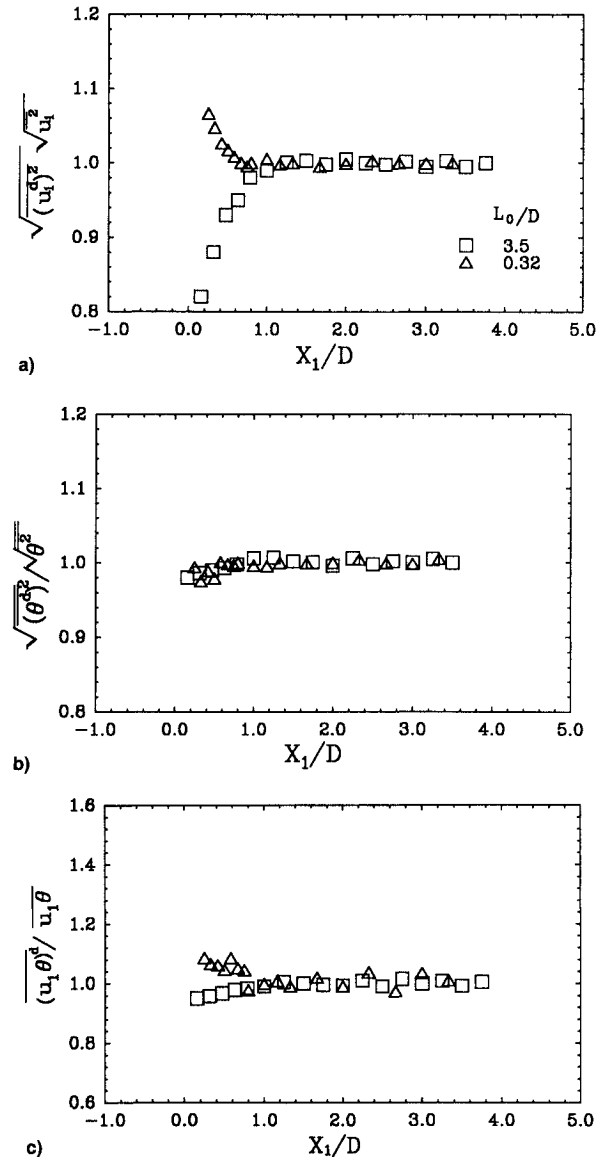


Fig. 2 Variation of the normalized a) rms velocity, b) rms temperature, and c) axial heat flux for flow along $y = D/2$. (Uncertainties are the same as Fig. 1.)

on the scalar field are quantitatively similar. This indicates that outside the region where the blockage effect is significant, the passive scalar is unaffected by the strain regardless of the magnitude and direction of the strain.

For $L_0/D = 0.32$ near the stagnation point, vortex stretching causes an increase in the magnitude of the turbulent axial heat flux. At the station nearest to the stagnation point, the distorted axial heat flux is 1.8 times its undistorted value at the same location and experimental conditions. Due to the blockage effect, the axial heat flux for $L_0/D = 3.5$ at the nearest station to the stagnation point is about 40% less than its undistorted value. The variation in the axial heat flux for axisymmetric objects for different L_0/D ratios is qualitatively similar to the corresponding results for the two-dimensional objects. However, since the effect of distortion is less than that for the two-dimensional objects, the amount of attenuation and amplification in the normalized heat flux is less and occurs closer to the stagnation point than for the two-dimensional objects.

Figures 2a–c show the variation of the same quantities as given in Fig. 2 along a line parallel to the edge of the objects ($y = D/2$). The increase and decrease in these quantities are similar but less than the corresponding quantities along the mean stagnation streamline.

References

- ¹Hunt, J. C. R., "A Theory of Two-Dimensional Flow Round Two-Dimensional Bluff Bodies," *Journal of Fluid Mechanics*, Vol. 61, Pt. 4, Dec. 1973, pp. 625–706.
- ²Bearman, P. W., "Some Measurement of Distortion of Turbulence Approaching a Two-Dimensional Bluff Body," *Journal of Fluid Mechanics*, Vol. 53, Pt. 2, June 1972, pp. 451–467.
- ³Britter, R. E., Hunt, J. C. R., and Mumford, J. C., "The Distortion of Turbulence by a Circular Cylinder," *Journal of Fluid Mechanics*, Vol. 92, Pt. 2, May 1979, pp. 269–301.
- ⁴Rahai, H., and LaRue, J. C., "Effect of Flow Distortion on a Turbulent Scalar Field," *Seventh Symposium on Turbulent Shear Flows*, Stanford, CA, Aug. 1989, pp. 14.3.1–14.3.6.
- ⁵Wynngaard, J. C., Rockwell, L., and Friehe, C., "Errors in the Measurement of Turbulence Upstream of an Axisymmetric Body," *Journal of Atmosphere and Ocean Technology*, Vol. 5, No. 2, 1985, pp. 605–614.
- ⁶LaRue, J. C., Deaton, T., and Gibson, C. H., "Measurement of High Frequency Turbulent Temperature," *Review of Scientific Instruments*, Vol. 46, No. 6, 1975, pp. 757–763.
- ⁷Rahai, H. R., and LaRue, J., "Errors in the Measurements of Turbulent Scalar Upstream of Axisymmetric Objects," AIAA Paper 90-1591, June 1990.

Quantifying Thermal Radiation and Convection Effects During Constant-Heat-Flux Irradiation

Terry J. Hendricks*

University of Texas at Austin, Austin, Texas 78758

Nomenclature

- C_p = specific heat, J/kg-K
 \bar{H} = nondimensional thermal convection parameter, $(hT_i)/(\alpha_n I)$

- h = thermal convection coefficient, W/m²-K
 I = laser intensity, environmental heat flux, W/cm²
 T_a = ambient temperature, K
 T_i = initial temperature, K
 T_{max} = maximum temperature before material breakdown, K
 t = time, s
 t_{max} = maximum exposure time before material breakdown, s
 x = depth, m
 α_n = total or spectral normal surface absorptivity
 β = semi-infinite wall parameter, K/s^{1/2} – $(2\alpha_n I)/(\rho C_p \lambda \pi)^{1/2}$
 δ = wall thickness, m
 ϵ = total hemispherical surface emissivity
 η = thin wall parameter, K/s – $(\alpha_n I)/(\rho C_p \delta)$
 θ_{max} = maximum nondimensional temperature, $(T_{max} - T_i)/T_i$
 θ_n = n th-order nondimensional perturbation temperature, $\Delta T_n/T_i$
 θ_0 = 0th-order nondimensional temperature, $(T_0 - T_i)/T_i$
 κ = thermal diffusivity, m²/s – $\lambda/(\rho C_p)$
 λ = thermal conductivity, W/m-K
 ξ = nondimensional depth, $x/(\kappa t)^{1/2}$
 ρ = density, kg/m³
 σ = Stephan-Boltzmann constant, W/m²-K⁴
 χ = nondimensional thermal radiation parameter, $(\sigma \epsilon T_i^4)/(\alpha_n I)$
 ψ_n = nondimensional time parameter, $(\eta t/T_i)$, $(\beta t^{1/2}/T_i)$

Introduction

MATERIAL survivability during constant-heat-flux irradiation is of increasing importance to many defense and commercial applications. Spacecraft and laser weaponry design are major defense applications concerned with material survivability during high-intensity laser irradiation of both ground-based and space-based systems. Commercial applications where material survivability is important include, inertial confinement fusion (ICF) reactor design, Tokamak fusion reactor design, many types of laser-driven materials processing, and thermal protection system (TPS) design in high-velocity planetary re-entry vehicles.

It is often desirable and necessary to have estimates of thermal reradiation and convection effects on material transient thermal response and survivability characteristics during constant-heat-flux irradiation. Although transient thermal response of irradiated materials can be impacted by thermal reradiation and convection conditions at the material surface, little analytical work includes thermal reradiation and convection effects in a closed-form analytic solution. Several references^{1–4} discuss analytic solutions to thin-wall, thick-wall, and semi-infinite wall analysis cases, assuming no thermal radiation and convection from the material surface. Abarbanel,⁵ Bartholomeusz,⁶ and Chen et al.⁷ have investigated analytic treatment of thermal conduction in finite-thickness and semi-infinite cooling solids, but not with the combination of incident irradiation, thermal reradiation, and thermal convection at the surface. Roy et al.,⁸ Modest et al.,^{9,10} Yuen et al.,¹¹ and Knight¹² effectively treated such complexities as three-dimensional effects, pulsed and moving beams, in-depth absorbing, emitting, and scattering effects on transient heating, and vaporization using numerical techniques, but neglected thermal reradiation and convection effects. This work presents a rapid, accurate analytic methodology to evaluate first-order thermal reradiation and convection impacts on material survivability before breakdown (i.e., ablation, melting) during constant-heat-flux irradiation.

Many constant-flux thermal response problems can be effectively analyzed, at least to a first approximation, with a one-dimensional thermal analysis. This approach is particularly applicable to situations where lateral thermal conduction

Received April 3, 1992; revision received Aug. 13, 1992; accepted for publication Aug. 14, 1992. Copyright © 1992 by the American Institute of Aeronautics and Astronautics, Inc. All rights reserved.

*Ph.D. Candidate, University Fellow, Department of Mechanical Engineering, Center for Energy Studies, 10100 Burnet Road. Member AIAA.